



# 1 **Ubiquitous increases in flood magnitude in the Columbia River** 2 **Basin under climate change**

3 Laura E. Queen<sup>1</sup>, Philip W. Mote<sup>1</sup>, David E. Rupp<sup>1</sup>, Oriana Chegwiddden<sup>2</sup>, and Bart Nijssen<sup>2</sup>

4

5

6 <sup>1</sup>Oregon Climate Change Research Institute, Oregon State University, Corvallis OR 97331 USA

7 <sup>2</sup>Department of Civil and Environmental Engineering, University of Washington Seattle WA 98105 USA

8 *Correspondence to:* Laura Queen (lqueen@uoregon.edu)

9 **Abstract.** The US and Canada have entered negotiations to modernize the Columbia River Treaty, signed in 1961.  
10 Key priorities are balancing flood risk, hydropower production, and improving aquatic ecosystem function while  
11 incorporating projected effects of climate change. In support of the US effort, Chegwiddden et al. (2017) developed  
12 a large-ensemble dataset of past and future daily flows at 396 sites throughout the Columbia River Basin (CRB)  
13 and select other watersheds in western Washington and Oregon, generating a large ensemble using state-of-the  
14 art climate and hydrologic models. In this study, we use that dataset - the largest now available - to present new  
15 analyses of the effects of future climate change on flooding using water year maximum daily flows. For each  
16 simulation, flood statistics are estimated from Generalized Extreme Value distributions fit to simulated water year  
17 maximum daily flows for 50-year windows of the past (1950-1999) and future (2050-2099) periods. Our results  
18 contrast with previous findings: we find that the vast majority of locations in the CRB are estimated to experience  
19 an increase in future discharge magnitudes. We show that on the Columbia and Willamette rivers, increases in  
20 discharge magnitudes are smallest downstream and grow larger moving upstream. For the Snake River, however,  
21 the pattern is reversed, with increases in discharge magnitudes growing larger moving downstream to the  
22 confluence with the Salmon River tributary, and then abruptly dropping. We decompose the variation in results  
23 attributable to climate and hydrologic factors, finding that climate contributes more variation in larger basins  
24 while hydrology contributes more in smaller basins. Equally important for practical applications like flood control  
25 rule curves, the seasonal timing of flooding shifts dramatically on some rivers (e.g., on the Snake, 20th century  
26 floods occur exclusively in late spring, but by the end of the 21st century some floods occur as early as December)  
27 and not at all on others (e.g. the Willamette).



28

## 29 **1 Introduction**

30 Among natural disasters in the Northwest, flooding ranks second behind fire in federal disaster declarations<sup>1</sup> since  
31 1953 despite extensive flood prevention infrastructure. The largest flood in modern times on the Columbia  
32 occurred in late spring (May-June) 1948, and obliterated the town of Vanport which lay on an island between  
33 Portland, OR and Vancouver, WA, permanently displacing its 18,500 residents<sup>2</sup>. Other disruptive floods in the  
34 region include the Heppner flood in 1903, one of the deadliest flash floods in US history (Byrd, 2014); floods on  
35 the Chehalis River in both December 2007<sup>3</sup> and January 2009<sup>4</sup> that closed Interstate 5, the main north-south  
36 transportation corridor through the Northwest, for several days each time at a cost of several \$m per day to freight  
37 movement alone; and floods on the Willamette River in February 1996 and April 2019. The timing of typical  
38 floods varies widely across the region: low-elevation basins in western Washington and Oregon typically flood  
39 in November through February, whereas the snow-dominant basins east of the Cascades more typically flood in  
40 spring, even as late as June (Berghuis et al. 2016).

41  
42 The Columbia River drains much of the Northwest, with the fourth largest annual flow volume in the US and a  
43 drainage that includes portions of seven states plus the Canadian province of British Columbia (BC). Its numerous  
44 federal and nonfederal dams provide flood protection, hydropower production, navigation, irrigation, and  
45 recreation services. A treaty with Canada, signed in 1961, codified joint management of the river's reservoirs (and  
46 funded construction of new reservoirs in BC) primarily to provide flood protection and hydropower production<sup>5</sup>.  
47 The US and Canada have entered negotiations to update the treaty; the USA's "key objectives include continued,  
48 careful management of flood risk; ensuring a reliable and economical power supply; and improving the ecosystem  
49 in a modernized Treaty regime." (*ibid.*) Both countries have expressed an intention to include the effects of climate  
50 change on flows, and clearly a key aspect of hydrologic change is to inform the treaty negotiations of the influence  
51 of climate change on the magnitude of flooding.

---

<sup>1</sup> <https://www.fema.gov/data-visualization-summary-disaster-declarations-and-grants> accessed 8/6/2019

<sup>2</sup> [https://www.oregonlive.com/portland/2017/05/vanport\\_flood\\_may\\_30\\_1948\\_chan.html](https://www.oregonlive.com/portland/2017/05/vanport_flood_may_30_1948_chan.html) accessed 8/6/2019

<sup>3</sup> <https://www.seattletimes.com/seattle-news/extensive-flooding-3-confirmed-deaths-hundreds-of-rescues/>  
accessed 8/6/2019

<sup>4</sup> <https://www.seattletimes.com/seattle-news/despite-drying-cooling-trend-flooding-and-road-closures-continue/>  
accessed 8/6/2019

<sup>5</sup> <https://www.state.gov/columbia-river-treaty/> accessed 8/6/2019



52

53 While rising temperatures potentially affect all parts of the hydrologic cycle, in a snowmelt-dominated hydrologic  
54 system such as many of the Northwest's rivers, warming directly affects snow accumulation and melt.  
55 Observational studies have shown consistent changes toward lower spring snowpack (Mote et al. 2018), earlier  
56 spring flow (Stewart et al. 2005), and lower summer flow (Fritze et al. 2011) since the mid-20th century.  
57 Observations of trends in flooding in the US have generally failed to find any consistent trends (Lins and Slack  
58 1999; Douglass et al. 2000; Sharma et al. 2018). Sharma et al. (2018) offer several possible explanations, chiefly  
59 "decreases in antecedent soil moisture, decreasing storm extent, and decreases in snowmelt". The detection of  
60 trends in floods is complicated by the interaction of extreme events and nonstationarity (Serinaldi and Kilsby,  
61 2015). Moreover, as a result of the substantial alteration of rivers to prevent flooding (e.g., by the construction of  
62 dams and levees) during the observational period, the best long-term records - i.e., on streams with the least  
63 modifications - are on rivers that were not producing sufficiently disruptive floods to lead decision-makers to  
64 construct flood protection structures.

65

66 To interpret the ambiguous results from observed trends, Hamlet and Lettenmaier (2007) used the Variable  
67 Infiltration Capacity (VIC) hydrologic model forced twice with detrended observed daily weather for the period  
68 1916-2003, with about 1°C of temperature difference between the two. They then compared 20- and 100-year  
69 flood quantiles for basins at varying sizes in the western US and found a wide range of changes in flood magnitude  
70 ranging from large decreases to large increases (+/- 30%). Broadly, the responses depended somewhat on basin  
71 winter temperature, with the coldest basins (<-6°C) showing reductions in flood magnitude owing to reduced  
72 snowpack, basins with moderate temperatures exhibiting a wide range of changes, and rain-dominant (>5°C)  
73 basins showing little change, though the warm basins in coastal areas of Washington, Oregon, and California  
74 showed increased flood magnitude.

75

76 Modeling work using state-of-the-art hydrologic models has been applied to understand where and how flood  
77 magnitudes may change in the future. Tohver et al (2014) found widespread increases in flood magnitudes,  
78 especially in temperature-sensitive basins (mainly on the west side of the Cascades), but their approach used  
79 monthly GCM output so changes in daily precipitation would not be represented. Salathé et al. (2014) used a  
80 single global climate model (GCM), the ECHAM5, linked to a regional climate model to obtain high-resolution  
81 (in space and time) driving data for VIC over the period 1970-2069. As did Hamlet and Lettenmaier (2007), they  
82 compared the ratio of flood change (2050s vs 1980s) against mean historical winter temperature and found a



83 majority of locations with a higher 100-year flood, in some cases by a factor of 2 or more; while they projected  
84 increases in every one of the warmer basins ( $>0^{\circ}\text{C}$ ), a substantial fraction of colder locations had decreases in  
85 flood magnitude.

86

87 As noted above and detailed below, Chegwiddden et al. (2019) describe the process used to generate the streamflow  
88 ensemble used here. In addition, they used analysis of variance (ANOVA) to analyze the different influences of  
89 choices of emissions scenario (as a Representative Concentration Pathway - RCP), GCM, downscaling method,  
90 and hydrologic model, and how those influences varied spatially across the domain and also seasonally and by  
91 hydrologic variable. They found that the RCP and GCM had the largest influence on the range of annual  
92 streamflow volume and timing, and hydrologic model had the largest influence on low flows. The hydrologic  
93 variables they considered were snowpack (maximum snow water equivalent and date of maximum SWE), annual  
94 streamflow volume, centroid timing (the date at which half the water year's flow has passed), and seasonal  
95 streamflow volume; primary focus was on centroid timing, annual volume, and minimum 7-day flow. They did  
96 not examine maximum daily flow, which is the purpose of this paper.

## 97 **2 Methods**

### 98 **2.1 Hydrologic modeling data set**

99 To assess changing flood magnitudes under climate change, we analyzed changes in water year maximum daily  
100 flows in a large ensemble of streamflow simulations at 396 locations in the CRB (Figure MAP) and select  
101 watersheds in western Oregon and Washington (Chegwiddden et al., 2017). The simulations were constructed from  
102 permutations of modeling decisions on forcing datasets and hydrologic modeling. Specifically, choices included  
103 two RCPs (RCP4.5 and RCP8.5), ten GCMs, two methods of downscaling the climate model output to the  
104 resolution of the hydrologic models, and four hydrologic model implementations, for a total of 160 permutations.  
105 For our analysis, we extracted a more tractable dataset of 40 simulations per location, by only considering  
106 simulations with RCP 8.5 and the Multivariate Adaptive Constructed Analogs (MACA) downscaling method  
107 (Abatzoglou and Brown, 2012).

108

109 The rationale for using a subset of the available data is as follows. First, the time-dependent set of greenhouse gas  
110 concentrations in RCP4.5 is fully included in RCP8.5, so any concentration of greenhouse gases on the RCP4.5  
111 path can be converted to a point on RCP8.5 (at a different time). We analyzed results for both RCP8.5 and RCP4.5,



112 and found that to first order the changes in flood magnitude in RCP4.5 were approximately 2/3 those in RCP8.5,  
113 which is also roughly the ratio of global temperature change over the period considered (IPCC Summary for  
114 Policymakers, 2014). For clarity we show only the results for RCP8.5. Second, we considered only simulations  
115 using the MACA downscaling method because of the method's ability to capture the daily GCM-simulated  
116 meteorology critical for assessing changes in extremes and its skill in topographically complex regions (Lute et  
117 al., 2015). The other downscaling approach used by Chegwiddden et al. (2019), the Bias Correction and Statistical  
118 Downscaling (BCSD) method (Wood et al. 2004), produces probability distributions of daily precipitation  
119 inconsistent with the GCM response to forcings because the method stochastically disaggregates monthly data to  
120 daily data based on historical statistical properties of the daily data. This statistical property limits the ability of  
121 BCSD to reproduce changes in storm frequency in the future, making it a less attractive choice for daily extreme  
122 flow analysis (Hamlet et al. 2010; Guttman et al. 2014).

123  
124 The GCMs used in this study are the CanESM2, CCSM4, CNRM-CM5, CSIRO-Mk3-6-0, GFDL-ESM2M,  
125 HadGEM2-CC, HadGEM2-ES, Inmcm4, IPSL-CM5A-MR, and MIROC5. These ten GCMs were chosen  
126 primarily for their ability to accurately reproduce observed climate metrics during the historical period mainly of  
127 the Northwest US but also at sub-continental and larger scales as assessed in Rupp et al. (2013) and RMJOC  
128 (2018). The four hydrologic model implementations included two distinct hydrologic models: the Variable  
129 Infiltration Capacity (VIC; Liang et al., 1994) model and the Precipitation Runoff Modeling System (PRMS;  
130 Leavesley et al., 1983). VIC and PRMS are process-based, energy balance models and were both run on the same  
131 1/16th degree grid with output saved at a daily time step for the period 1950 to 2099. VIC also included a glacier  
132 model (Hamman & Nijssen, 2015). Three unique implementations of VIC were used with independently derived  
133 parameter sets (P1, P2, P3) marked by differences in calibrated parameters, calibration methodology, and  
134 meteorological and streamflow reference sets. See Chegwiddden et al (2019) for details. It is important to note that  
135 these hydrologic simulations and calibrations do not include reservoir models.

## 136 **2.2 Flood magnitude**

137 We assessed changes in flood magnitude in the Columbia River Basin by comparing maximum daily streamflows  
138 over a 150-year period (1950-2100). We estimated the 10, 5, 2, and 1% probability of occurrence (commonly  
139 referred to as the 10-, 20-, 50-, and 100-year flood, respectively) by fitting generalized extreme value (GEV)  
140 probability distributions to simulated water year maximum daily flows for 50-year windows of the past (1950-  
141 1999) and future (2050-2099) periods. (We also looked at 30- and 75-year windows, choosing 50 years as a



142 balance between sample size favoring longer periods, and nonstationarity considerations favoring shorter periods.)  
143 We used Python's `scipy.stats.genextreme` module (Jones et al., 2001) to fit a Gumbel distribution and estimate  
144 flood magnitudes for each return period. We assessed change in flood magnitude as the “discharge ratio” of the  
145 estimated future to past floods for a given return period; a ratio greater than 1 indicates an increase in flood  
146 magnitudes while a ratio less than 1 indicates a decrease.

147  
148 We describe how changes in flood magnitude vary by climatic zone across the PNW by using an efficient and  
149 internally consistent proxy for climatic zone: the centroid of timing – the day in the water year that half the annual  
150 volume of water has passed through the location. The centroid of timing is a metric of snow dominance (e.g.,  
151 Stewart et al. 2005) which is related to the spatial distribution of temperature and tends to decrease downstream.  
152 This temporal proxy of a hydrologic characteristic is effective in the Columbia Basin where most of the  
153 precipitation occurs in winter and the relative magnitude and timing of the freshet from the spring thaw is a good  
154 indicator of importance of snowmelt to streamflow. An early centroid indicates that rain, which falls  
155 predominantly during the cooler, earlier part of the year, is the driver of the peak flows at the location, while a  
156 late centroid indicates that snowmelt during later spring months is the prime hydrological driver. We computed  
157 the centroid using the 1950-79 simulated years. Note that Chegwiddden et al. (2019) also used the *change* in  
158 centroid as a hydrologic variable of interest; below, we discuss our results in the context of their findings.

## 159 **3 Results**

### 160 **3.1 Regional changes in flood ratio**

161 Figure 3 shows the changes in maximum daily discharge for all of the 396 flow locations for different return  
162 periods. The horizontal position of each circle represents the centroid of timing. The circles are semi-opaque so  
163 overlapping circles lead to a deeper saturation. Each circle represents the average of the ratios of change for the  
164 40 hydrological simulations for that location. (In Figure 5 we will show the full set of points for select locations.)  
165 Points on the same river tend to be ordered from more to less snow dominant traveling downstream; strings of  
166 circles in a smooth pattern sometimes indicate points on a given river, and a few of these are highlighted in Figure  
167 4.

168  
169 A striking result in Figure 3 is that the flood magnitude increases (i.e., the discharge ratio exceeds one) at nearly  
170 every flow location and return period (though not for every individual climate scenario, as shown in Figure 5).



171 Broadly, the patterns are similar across all return periods though with slightly higher ratios for longer return  
172 periods, and subsequent figures will show only the 10- and 100-year floods. For the flow locations with centroid  
173  $<125$  or so (i.e. February 2), flood ratios are fairly concentrated about 1.25 for all return periods. For mixed rain-  
174 snow basins, roughly delineated by centroids between 125 and 160 (March 8 most years), flood ratios range widely  
175 from just below 1 to about 2.4 for the 10-year and 3.2 for 50- and 100-year floods. For the longer return intervals,  
176 there is a wide range of projected changes in daily flood at many locations (indicated by the red coloring). This is  
177 undoubtedly partly due to the GEV fit extrapolating from 50 to 100 years. Finally, for the basins with flow centroid  
178  $>160$ , the ratios have a smaller range, from slightly greater than 1 to a maximum that increases from about 2 for  
179 the 10-year, to about 2.75 for 100-year.

180

181 To understand better how flood magnitude changes along the length of a river, we focus (Figure 4) on a handful  
182 of significant rivers in the region: the mainstem Columbia, Willamette (along with major tributaries the McKenzie  
183 and Middle Fork Willamette), and Snake, and also on the Chehalis in southwest Washington (see Introduction).  
184 Flow locations are listed in Table 3 Rivers in the Appendix. The Columbia River includes the most snow-dominant  
185 basins, with a centroid of  $>190$  days (early to mid April) in the Canadian portion of the basin. The flood ratio  
186 decreases almost uniformly along the length of the river, from 1.3 for the 10-year and  $>1.5$  for the 100-year in the  
187 Canadian portion to just above 1 at the last few points along the river (The Dalles, Bonneville, and Portland). Like  
188 the Columbia, the Willamette also has flood ratios that decrease along the length of the river, from 1.7 to 1.35 for  
189 both return periods. The McKenzie River (points 15-17), one of the three tributaries that converge at Eugene to  
190 form the Willamette, is a highly aquifer-fed river with higher baseflow than is represented in the hydrologic  
191 models, though it is unclear how that difference would manifest in the flood statistics.

192

193 Surprisingly, the Snake behaves oppositely: flood ratio increases along the length of the river, until the confluence  
194 with the Salmon River, which drains a large mountainous area of central Idaho. On parts of the Snake the ratios  
195 are as high as 1.4 for 10-year and 1.6 for 100-year. Then after the confluence with the Salmon River, which has  
196 much lower change in discharge ratio, the ratios on the Snake drop to about 1.2 for 10-year and about 1.3 for the  
197 100-year. Our hypothesis is that in the Snake above the Salmon River, the tributaries shift from snow-dominant  
198 to rain-dominant, so that a single storm can drive large rainfall-driven increases (possibly with a snowmelt  
199 component) leading to larger synchronous discharges. The Salmon and Clearwater rivers retain less exposure to  
200 such shifts, and dilute the effects of single large storms on flooding. Fully understanding the reasons for this  
201 curious behavior would require additional analysis, beyond the scope of this paper.



202

203 Each circle in Figures 3 and 4 represents an average of 40 simulations: 10 GCMs and 4 hydrologic model  
204 configurations. To better understand the range in results, Figure 5 shows the discharge ratio for all 40 simulations  
205 at each point on the mainstem Columbia. Although the mean flood ratio at the lowest two points is only barely  
206 above 1, several ensemble members have ratios less than one, and a few have ratios  $>1.5$ . Moving upstream, the  
207 range in results increases, as shown also by the color of the dots.

### 208 **3.2 Dependence of results on modeling choices**

209 As in Chegwiddden et al (2019), we separate the results - here for the three largest rivers - into variations across  
210 GCM (Figure 6) and variations across hydrologic model configurations (Figure 7). The ranking of flood ratios by  
211 GCM changes substantially between basins and even within a basin, and does not correspond to the changes in  
212 seasonal precipitation. For the upper Columbia River, the models with the least warming - inmcm4 and GFDL-  
213 ESM2M (Rupp et al 2017) - have almost no change in flood magnitude, but the HadGEM2-ES which warms  
214 considerably in summer produces a large decrease in flood magnitude. In the Willamette and Snake Rivers, the  
215 range of projected flood changes by different GCMs remains large from the headwaters to the mouth of the river,  
216 whereas for the Columbia the range diminishes considerably as one moves downriver.

217

218 The variation of results depends less on hydrologic model than on GCM (Figure 7), though the differences across  
219 hydrological models are still substantial. For the Willamette, lower Snake, and both upper and lower Columbia,  
220 the PRMS model predicts substantially larger increases in flooding than the three calibrations of the VIC model.  
221 For the upper Snake, it predicts substantially smaller change than any VIC calibration. While it is perhaps not  
222 surprising that the three calibrations of VIC are close to each other, it is striking just how different are the  
223 projections from PRMS at most locations on these three rivers. Chegwiddden et al. (2019) found that the main  
224 contributors to differences in hydrologic variables generally (except low flows) were the climate scenarios (GCM  
225 and RCP), consistent with our findings here. (The order of models is similar in the equivalent figure for the 100-  
226 year return period, but we elected to show the 10-year figure since the 100-year figure is more difficult to decipher  
227 because the symbols overlap with those from other rivers.)

228

229 To parse the contributions of climate factors (represented by the GCMs) and hydrologic factors (represented by  
230 the hydrologic models), we perform ANOVA on the 40 discharge ratios. The pie charts in Fig. 8 show the  
231 proportion of the total variance explained by climate factors and hydrologic factors at different locations. For the





232 Willamette River, the role of climate grows more important and the role of hydrologic variability less important  
233 going from the confluence of the three major tributaries at Eugene to the mouth. For the Snake and Columbia  
234 rivers, climate is responsible for virtually all of the variance in projections in the upper reaches, but only about  
235 half at the lowest point, similar to the Willamette. The Willamette basin is much smaller, and a large storm can  
236 affect the entire basin on the same day, whereas storms typically take a couple of days to move across the Snake  
237 and Columbia (and generally move upstream). With larger and more diverse contributing areas, differences in  
238 the rates with which the hydrological models transfer precipitation to the point of interest become more important.  
239 Unlike Chegwiddden et al. (2019), we did not attempt to isolate the response to anthropogenic forcing from internal  
240 climate variability. Though several techniques for separating these two factors have been used (e.g., Hawkins  
241 and Sutton, 2009; Rupp et al., 2017; Chegwiddden et al., 2019), these techniques are either infeasible with our  
242 dataset or we question their suitability for the application to changes in extreme river flows.  
243

### 244 **3.3 Change in timing**

245 Although in a broad hydrologic sense a flood is a flood regardless of what time of year it occurs, there are  
246 potentially significant ecological differences depending on time of year; for example, scouring salmon redds  
247 (Goode et al. 2013). Moreover, water management policies are strongly linked to the calendar year (see  
248 Discussion). We computed the probability of flooding for (all 40) past and future simulations at all the points on  
249 the three rivers (Figure 4) as a function of day of year (Figure 9). For the Willamette, no significant change in  
250 timing occurs; however, for the upper Willamette, a single peak in likelihood in February becomes more diffuse,  
251 whereas for the lower Willamette, a more diffuse distribution becomes more peaked. For the Snake, all locations  
252 see a shift toward earlier floods, consistent with the transition to less snow-dominant and more rain-dominant.  
253 Whereas floods were historically concentrated in the period of mid-May to mid-July, the projected future flooding  
254 period spans December to June. For the Columbia, the mode in the flood timing shifts earlier by half a month in  
255 the upper Columbia to about a month in the lower Columbia. The distribution also broadens with an elongated  
256 tail towards winter such that there is low, but non-negligible, probability of floods occurring as early as January.  
257 Although the magnitude of the 10- and 100-year flood events in the lower Columbia do not increase much (Figures  
258 4-7), the risk of major flood on any given day decreases, and the likelihood of major flooding in May or April (or  
259 even February and March) increases.



#### 260 **4 Discussion and conclusions**

261 Compared with Salathe et al. (2014), who found decreases in flooding at a substantial number of sites, our results  
262 show increases in flood magnitude at nearly every return period and location, which includes about 100 locations  
263 not included in their study. They also noted that directly downscaling the GCM outputs leads to a smaller range  
264 of results than when running the regional model as an intermediate step. In our study, the MACA statistical  
265 downscaling approach preserves much of the daily variability from the GCM, so the primary reason for the  
266 difference between our results and theirs is probably the fact that we analyzed 40 scenarios. Some locations, for  
267 example the points on the lower Columbia river, had a handful of ensemble members with decreasing flood  
268 magnitude. But averaging the entire ensemble nearly always resulted in a increase in flood magnitude. It is  
269 possible therefore that their study, repeated with a larger ensemble of hydrologic-climate model combinations,  
270 might have found ubiquitous increases in flood magnitude as ours did.

271  
272 Earlier results (Hamlet and Lettenmaier 2007, Tohver et al. 2014, Salathe et al. 2014) suggested a decrease in  
273 flood magnitude in snowmelt-dominated basins like the Columbia, since reduced snowpack reduces the store of  
274 water available to be released quickly in a spring flood (like the May-June 1948 Vanport flood). In a subbasin of  
275 the Willamette, Surfleet and Tullos (2013) projected decreases in flood magnitude for return periods > 10 years  
276 in the Santiam River basin under a high-emissions scenario (SRES A1B, 2070-2099 vs. 1960-2010; 8 GCMs),  
277 attributing the decreases to fewer large rain-on-snow events. Our results for the Santiam River show an *increase*  
278 of 40% for both 10- and 100-year floods; this result includes rain-on-snow events, since they are represented in  
279 VIC, which computes the accumulation of water in the snowpack and determines whether sufficient energy has  
280 been provided to create a melt event. Our results point to ubiquitous increases throughout the basin, even on the  
281 lower mainstem Columbia. The coldest basins including the headwaters of the Columbia also had some large  
282 increases in flood magnitude, suggesting that the former results were missing some key details. It seems likely  
283 that any reduction in flood magnitude originating from the warming-induced reduction in spring snowpack is  
284 offset by the increased pace of melt (including possibly rain-on-snow events). These results emphasize the  
285 necessity of revisiting reservoir rule curves, which are strongly tied to historical hydrographs, and also emphasize  
286 that changes in the seasonality of flooding can be dramatically different from the changes in the mean hydrograph.  
287 In particular, in the lower Snake and lower Columbia, changes in magnitude of flooding are modest but changes  
288 in timing of the earliest quartile of flood events is much larger than the 0.5-1 month shift in the mean hydrograph.  
289



290 A strength of our study compared with earlier studies is the use of our large ensemble. Conventional wisdom and  
291 evidence from the weather and seasonal climate forecasting realms illustrate the utility of considering ensembles,  
292 and that generally the true outcome of a prediction lies near the middle of the ensemble. The spread of results  
293 shown in Fig Col suggests that although the likeliest outcome is little change in flood magnitude in the lower  
294 Columbia, a prudent risk management strategy would consider the range of possibilities. However, we view the  
295 highest outcomes (>50% increase in peak 100-yr flood) as less likely than other individual scenarios, because  
296 they are the product of a hydrologic model that may be less suited to calculating the extreme changes in a much  
297 warmer world.

298  
299 Our findings provide an initial indication of how existing flood risk management could respond to a warming  
300 climate. Reservoir management is guided by rule curves which are intended to reflect the changing priorities and  
301 risks during the year. For example, reservoirs used for flood control have rule curves that require reservoir levels  
302 to be lowered when approaching the time of year when flood likelihood increases, and reservoir levels may be  
303 raised as the likelihood decreases. For the Willamette, we found little change in the distribution of timing of flood  
304 events, which indicate that with the state of the science today, reservoir rule curves may need to be altered as to  
305 magnitude of flooding (which our results indicate will increase by 30-40%) but not timing; a reservoir model  
306 would be required for complete understanding of how flood risk (magnitude and timing) will actually change. For  
307 the Snake, larger shifts in the timing imply a need to completely rethink the existing rule curves. For the Columbia,  
308 the mode in flood timing shifts earlier by half a month in the upper Columbia to about a month in the low  
309 Columbia. The distribution also broadens, with an elongated tail towards winter such that there is low, but non-  
310 negligible, probability of floods occurring as early as January. These changes in timing imply a need for moderate  
311 alteration of rule curves for reservoirs in the Canadian portion of the Columbia Basin.

312  
313 Our results should not be taken as a precise prediction of flood magnitude change but rather as the best available  
314 projections given the current state of the science. Two important factors need to be taken into account in  
315 interpreting our results: first, in using RCP8.5, we selected the most extreme emissions scenario. If efforts to  
316 stabilize the climate before 2050 are successful, the flood magnitudes shown here will undoubtedly be smaller  
317 (our analysis suggests most of the locations would see a change in flood magnitude about 1/3 smaller, for RCP4.5;  
318 e.g., a ratio of 1.3 (30% increase) for RCP8.5 would correspond to a ratio of 1.2 for RCP4.5).

319



320 The second important factor in interpreting our results is that the actual river system in the Northwest includes  
321 many dams, a majority of which have flood control as a primary (or one of a few top) objective. As a result, actual  
322 flows (and the changes in flow) at a given point in the river would be altered by reservoir management. Translating  
323 these changes in flood magnitude into actual changes would require a reservoir model for the basin or subbasin  
324 of relevance. One could then compute optimal rule curves for the major flood control reservoirs (perhaps time-  
325 evolving every couple of decades, to reflect the likely changes in scientific understanding and emissions  
326 trajectory). Even without that additional analysis, however, our results stress that the magnitude and/or timing of  
327 flood events will change throughout the basin. In other words, what worked for flood control in the past will not  
328 work as well in the future.

329  
330 This study may have some utility in framing and quantifying the possible changes in flood risk as the Columbia  
331 River Treaty is in renegotiation, but further work would be needed to assign probabilities to future flood  
332 magnitude. Such work includes (a) understanding whether the PRMS projections of much larger change are  
333 reliable, (b) applying different statistical and/or dynamical downscaling methods, and (c) using a more  
334 sophisticated approach to evaluating extremes in a nonstationary climate (as advocated by Serinaldi and Kilsby,  
335 2015). Furthermore, a new generation of GCM outputs (CMIP6, Eyring et al. 2016) already has data available  
336 from over 25 GCMs; in the near future, it would be feasible to apply a newer multi-model hydrologic modeling  
337 approaches (e.g., Clark et al., 2015) to the new generation of GCMs, though perhaps no significant changes would  
338 result. Nonetheless, with current knowledge the fact that very few locations would see a decrease in flood risk  
339 under any climate/hydrologic scenario is a strong statement of the need to update all aspects of flood preparation:  
340 the definition of N-year (especially 100-year) return period flows, flood plain mapping, and reservoir rule curves,  
341 to name a few. Moreover, the challenges that the renegotiated Columbia River Treaty faces in accounting for  
342 climate change now appear to include the necessity of incorporating the likely increase in flood risk throughout  
343 the region.

344  
345 **Code/data availability.** The data used here are available at <https://zenodo.org/record/854763>.

346  
347 **Author contribution.** L. Queen performed all analyses, wrote portions of the text, and edited the document. P.  
348 Mote guided the analysis and wrote much of the text. D. Rupp guided the analysis and edited the document. O.  
349 Chegwiddden generated the underlying dataset, guided the analysis, provided assistance with programming, and  
350 commented on the text. B. Nijssen generated the underlying dataset and commented on the text.



351

352 **Competing interests.** The authors declare no competing interests.

353

354 **Acknowledgments.** This project originated as a senior honors thesis by the first author, who thanks Hank Childs

355 of the University of Oregon for his mentorship. The research was supported by the NOAA Climate Impacts

356 Research Consortium, under award #NA15OAR4310145.

357



358

359

360 **References**

361

362 Berghuijs, W.R., R.A. Woods, C.J. Hutton, and M. Sivapalan, Dominant Flood Generating Mechanisms Across  
363 the United States. *Geophys. Res. Letts.*, 43, 4382-4390, doi: 10.1002/2016GL068070, 2016.

364

365 Byrd, J. G.: Calamity: The Heppner Flood of 1903. University of Washington Press, 2014.

366

367 Chegwiddden, O. S., B. Nijssen, D.E. Rupp, and P.W. Mote, Hydrologic Response of the Columbia River System  
368 to Climate Change [Data set]. Zenodo. doi:10.5281/zenodo.854763, 2017.

369

370 Chegwiddden, O. S., B. Nijssen, D.E. Rupp, J.R. Arnold, M.P. Clark, J.J. Hamman, S. Kao, et al: How Do Modeling  
371 Decisions Affect the Spread Among Hydrologic Climate Change Projections? Exploring a Large Ensemble of  
372 Simulations Across a Diversity of Hydroclimates. *Earth's Future*, 7, 623–637, doi: 10.1029/2018EF001047, 2019.

373

374 Clark, M. P., Nijssen, B., Lundquist, J. D., Kavetski, D., Rupp, D. E., Woods, R. A., ... & Arnold, J. R. (2015). A  
375 unified approach for process-based hydrologic modeling: 1. Modeling concept. *Water Resources Research*, 51(4),

376 2498-2514.

377

378 Do, H. X., F. Zhao, S. Westra, M. Leonard, L. Gudmundsson, J. Chang, P. Ciais, D. Gerten, S.N. Gosling, H.M.  
379 Schmied, T. Stacke, B.J.E. Stanislas, and Y. Wada: Historical and Future Changes in Global Flood Magnitude –  
380 Evidence from a Model-Observation Investigation. *Hydrol. Earth Syst. Sci. Discuss*, doi: 10.5194/hess-2019-388,  
381 in review, 2019.

382

383 Douglas, E.M., R.M. Vogel, and C.N. Kroll: Trends in Floods and Low Flows in the United States: Impact of  
384 Spatial Correlation. *Journal of Hydrology*, doi: 10.1016/S0022-1694(00)00336-X, 2000.

385



- 386 Eyring, V., S. Bony, G.A. Meehl, C.A. Senior, B. Stevens, R.J. Stouffer, and K.E. Taylor: Overview of the  
387 Coupled Model Intercomparison Project Phase 6 (CMIP6) Experimental Design and Organization. *Geosci. Model*  
388 *Dev.*, 9, 1937-1958, doi: 10.5194/gmd-9-1937-2016, 2016.
- 389
- 390 Fritze, H., I.T. Stewart, and E. J. Pebesma: Shifts in Western North American Snowmelt Runoff Regimes for the  
391 Recent Warm Decades. *Journal of Hydrometeorology*, doi: 10.1175/2011JHM1360.1, 2011.
- 392
- 393 Goode, J.R., J.M. Buffington, D. Tonina, D.J. Isaak, R.F. Thurow, S. Wenger, D. Nagel, C. Luce, D. Tetzlaff, and  
394 C. Soulsby: Potential effects of climate change on streambed scour and risks to salmonid survival in snow-  
395 dominated mountain basins. *Hydrological Processes*, 27, 750-765, doi: 10.1002/hyp.9728.
- 396
- 397 Gutmann, E., T. Pruitt, M. P. Clark, L. Brekke, J.R. Arnold, D. A. Raff, and R.M. Rasmussen: An Intercomparison  
398 of Statistical Downscaling Methods Used for Water Resource Assessments in the United States. *Water Resources*  
399 *Research*, 50, 7167–7186, doi: 10.1002/2014WR015559, 2014.
- 400
- 401 Hamlet, A.F., and D.P. Lettenmaier: Effects of 20th Century Warming and Climate Variability on Flood Risk in  
402 the Western U.S. *Water Resour. Res.*, 43, W06427, doi: 10.1029/2006WR005099, 2007.
- 403
- 404 Hamlet, A.F., E.P. Salathé, and P. Carrasco: Statistical Downscaling Techniques for Global Climate Model  
405 Simulations of Temperature and Precipitation with Application to Water Resources Planning Studies. Chapter 4  
406 in Final Report for the Columbia Basin Climate Change Scenarios Project, Climate Impacts Group, Center for  
407 Science in the Earth System, Joint Institute for the Study of the Atmosphere and Ocean, University of Washington,  
408 Seattle, 2010.
- 409
- 410 Hamman, J., and B. Nijssen: VIC 4.2.glaacier. Retrieved from [https://github.com/UW-](https://github.com/UW-Hydro/VIC/tree/support/VIC.4.2.glaacier)  
411 [Hydro/VIC/tree/support/VIC.4.2.glaacier](https://github.com/UW-Hydro/VIC/tree/support/VIC.4.2.glaacier), 2015.
- 412
- 413 Hawkins, E., and R. Sutton: The potential to narrow uncertainty in regional climate predictions. *Bulletin of the*  
414 *American Meteorological Society*, 90, 1095–1108, doi: 10.1175/2009BAMS2607.1, 2009.
- 415



- 416 Kundzewicz, Z.W., S. Kanae, S.I. Seneviratne, J. Handmer, N. Nicholls, P. Peduzzi, R. Mechler, L.M. Bouwer,  
417 N. Arnell, K. Mach, R. Muir-Wood, G.R. Brakenridge, W. Kron, G. Benito, Y. Honda, K. Takahashi, and B.  
418 Sherstyukov: Flood Risk and Climate Change: Global and Regional Perspectives. *Hydrological Sciences Journal*,  
419 59, 1-28, doi: 10.1080/02626667.2013.857411, 2014.
- 420
- 421 Lute, A. C., J.T. Abatzoglou, and K.C. Hegewisch: Projected Changes in Snowfall Extremes and Interannual  
422 Variability of Snowfall in the Western United States. *Water Resources Research*, 51, 960– 972, doi:  
423 10.1002/2014WR016267, 2015.
- 424
- 425 Najafi, M.R., and H. Moradkhani: Multi-model Ensemble Analysis of Runoff Extremes for Climate Change  
426 Impact Assessments. *Journal of Hydrology*, 525, 352-361, doi: 10.1016/j.jhydrol.2015.03.045, 2015.
- 427
- 428 River Management Joint Operating Committee: Climate and Hydrology Datasets for RMJOC Long-term Planning  
429 Studies. Second edition: Part 1—Hydroclimate Projections and Analyses, retrieved from  
430 <https://www.bpa.gov/p/Generation/Hydro/Pages/Climate-Change-FCRPS-Hydro.aspx>, 2018.
- 431
- 432 Rupp, D. E., J.T. Abatzoglou, K.C. Hegewisch, and P.W. Mote: Evaluation of CMIP5 20th Century Climate  
433 Simulations for the Pacific Northwest USA. *Journal of Geophysical Research: Atmospheres*, 118, 10,884–10,906,  
434 doi: 10.1002/jgrd.50843, 2013.
- 435
- 436 Rupp, D.E., J.T. Abatzoglou, and P.W Mote: Projections of 21st Century Climate of the Columbia River Basin.  
437 *Clim. Dyn.*, doi: 10.1007/s00382-016-3418-7, 2016.
- 438
- 439 Salathé, E. P., et al: Estimates of Twenty-First-Century Flood Risk in the Pacific Northwest Based on Regional  
440 Climate Model Simulations. *J. Hydrometeorol*, 15, 1881–1899, 2014.
- 441
- 442 Serinaldi, F., and C.G. Kilsby: Stationarity is Undead: Uncertainty Dominates the Distribution of Extremes.  
443 *Advances in Water Resources*, doi: 10.1016/j.advwatres.2014.12.013, 2015.
- 444

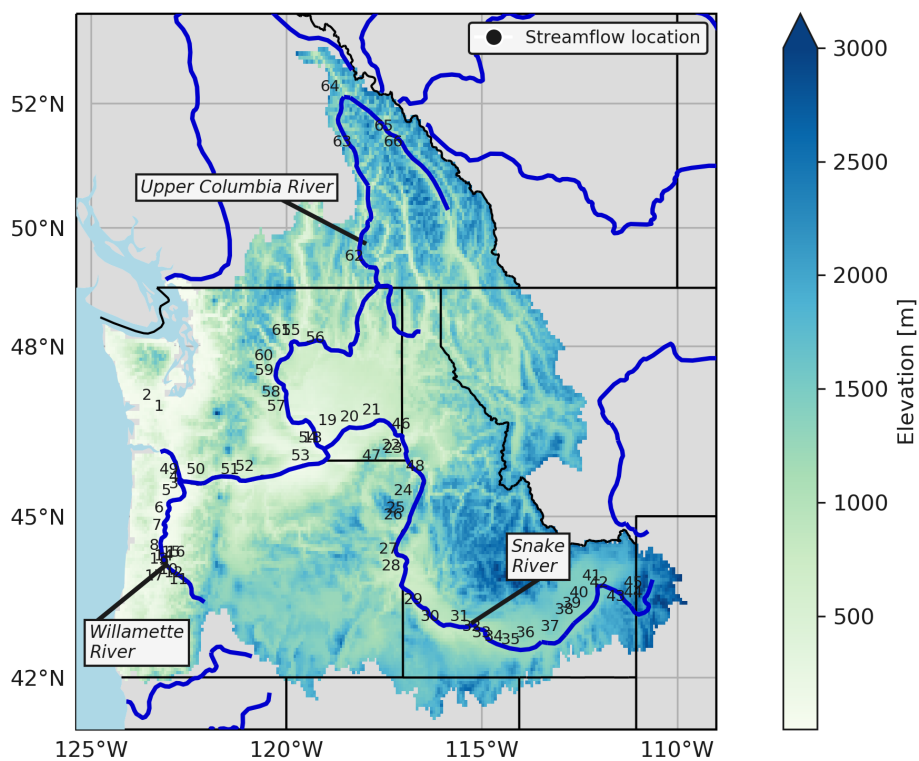




- 445 Sharma, A., C. Wasko, and D.P. Lettenmaier: If Precipitation Extremes Are Increasing, Why Aren't Floods? Water  
446 Resources Research, doi: 10.1029/2018WR023749, 2018.  
447
- 448 Stewart, I. T., D.R. Cayan, and M.D. Dettinger: Changes Toward Earlier Streamflow Timing Across Western  
449 North America. *J. Climate*, 18, 1136–1155, 2005.  
450
- 451 Surfleet, C. G., and D. Tullos, D.: Variability in Effect of Climate Change on Rain-on-Snow Peak Flow Events  
452 in a Temperate Climate. *Journal of Hydrology*, 479, 24-34, doi: 10.1016/j.jhydrol.2012.11.021, 2013.  
453
- 454 Tohver, I., A. F. Hamlet, and S.-Y. Lee: Impacts of 21st Century Climate Change on Hydrologic Extremes in the  
455 Pacific Northwest Region of North America. *J. Amer. Water Resour. Assoc.*, doi: 10.1111/jawr.12199, 2014.  
456
- 457 Vano, J. A., J. B. Kim, D. E. Rupp, and P. W. Mote: Selecting Climate Change Scenarios Using Impact-relevant  
458 Sensitivities. *Geophys. Res. Lett.*, 42, 5516–5525, doi: 10.1002/2015GL063208, 2015.  
459
- 460 Wood, A., L. Leung, V. Sridhar, and D. Lettenmaier: Hydrologic Implications of Dynamical and Statistical  
461 Approaches to Downscaling Climate Model Outputs. *Clim. Change*, 62, 189–216, 2004.  
462



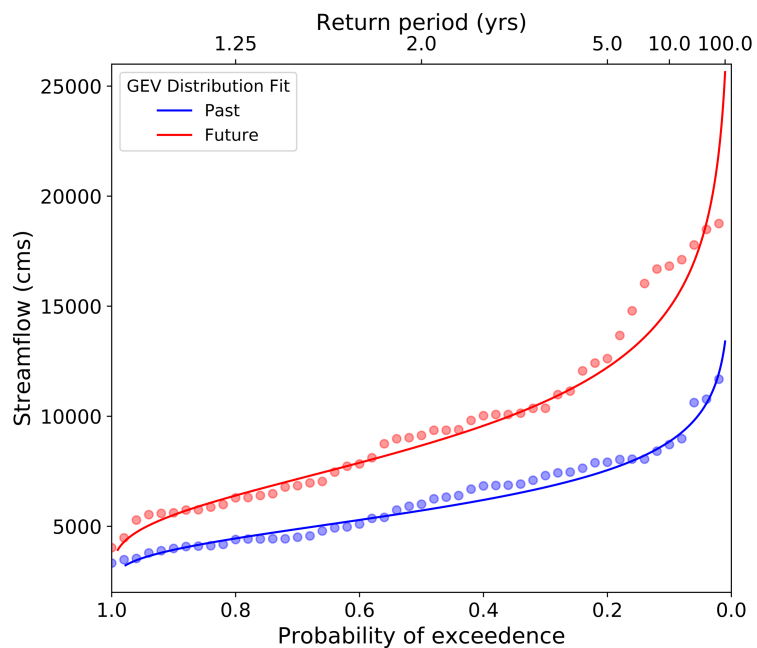
463



464 **Figure captions**

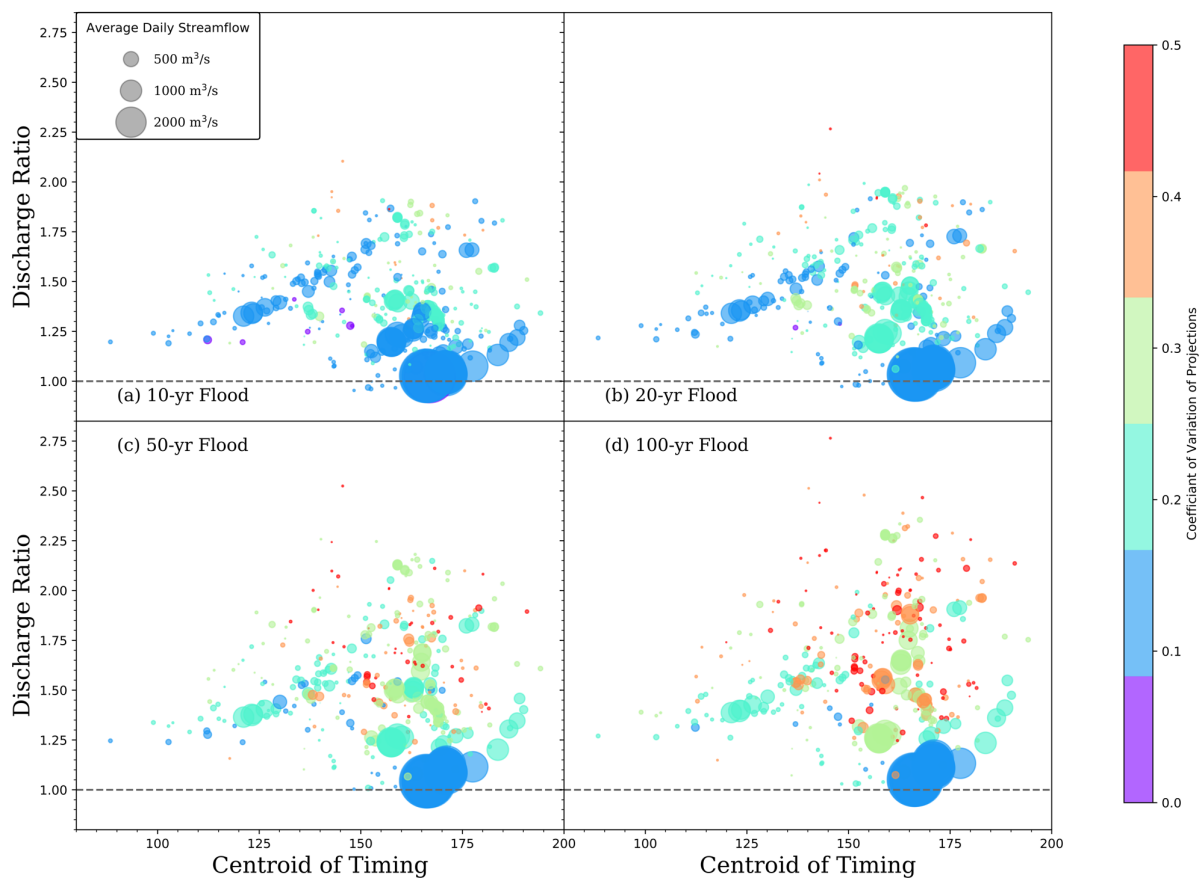
465

466 **Figure 1.** Domain of hydrologic simulations used in this paper, with colors indicating elevation of each grid cell,  
467 major rivers highlighted in blue, and numbers indicating locations of streamflow points highlighted in Figures 4-  
468 9, and Table 1. See Chegwiddden et al. (2017, 2019) for all streamflow locations plotted in Figure 3. Digital  
469 elevation data are in the public domain, obtained from <https://www2.usgs.gov/science/cite-view.php?cite=1530>



470

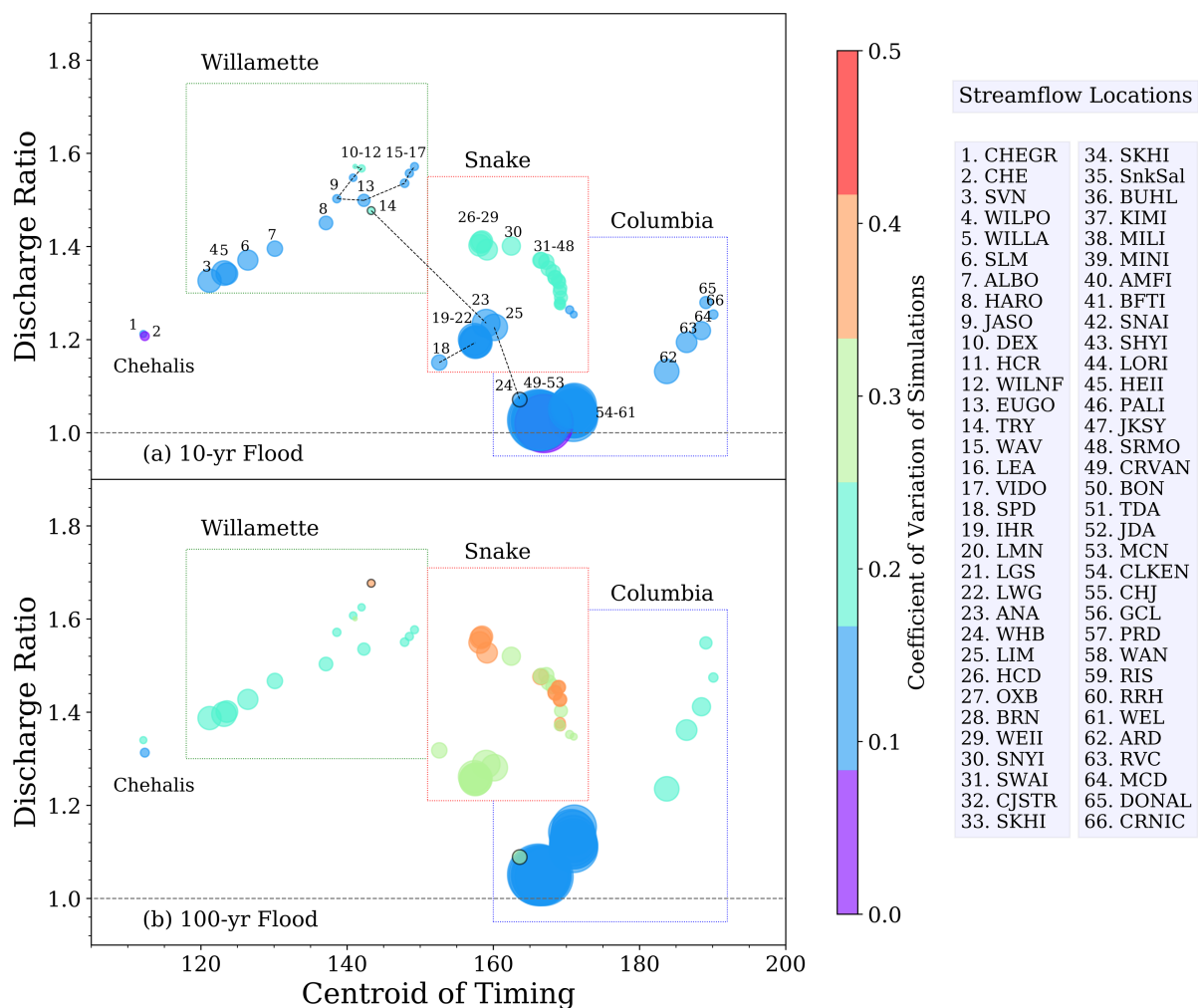
471 **Figure 2.** Generalized Extreme Value fit of annual maximum daily flow from 50 years of simulation using output  
472 from one GCM (HadGEM2-ES), one hydrologic model (PRMS), for the Willamette River at Portland. Red and  
473 blue dots/ lines indicate the annual values and GEV fit for the 1950-99 ‘past’ and 2050-99 ‘future’ periods.



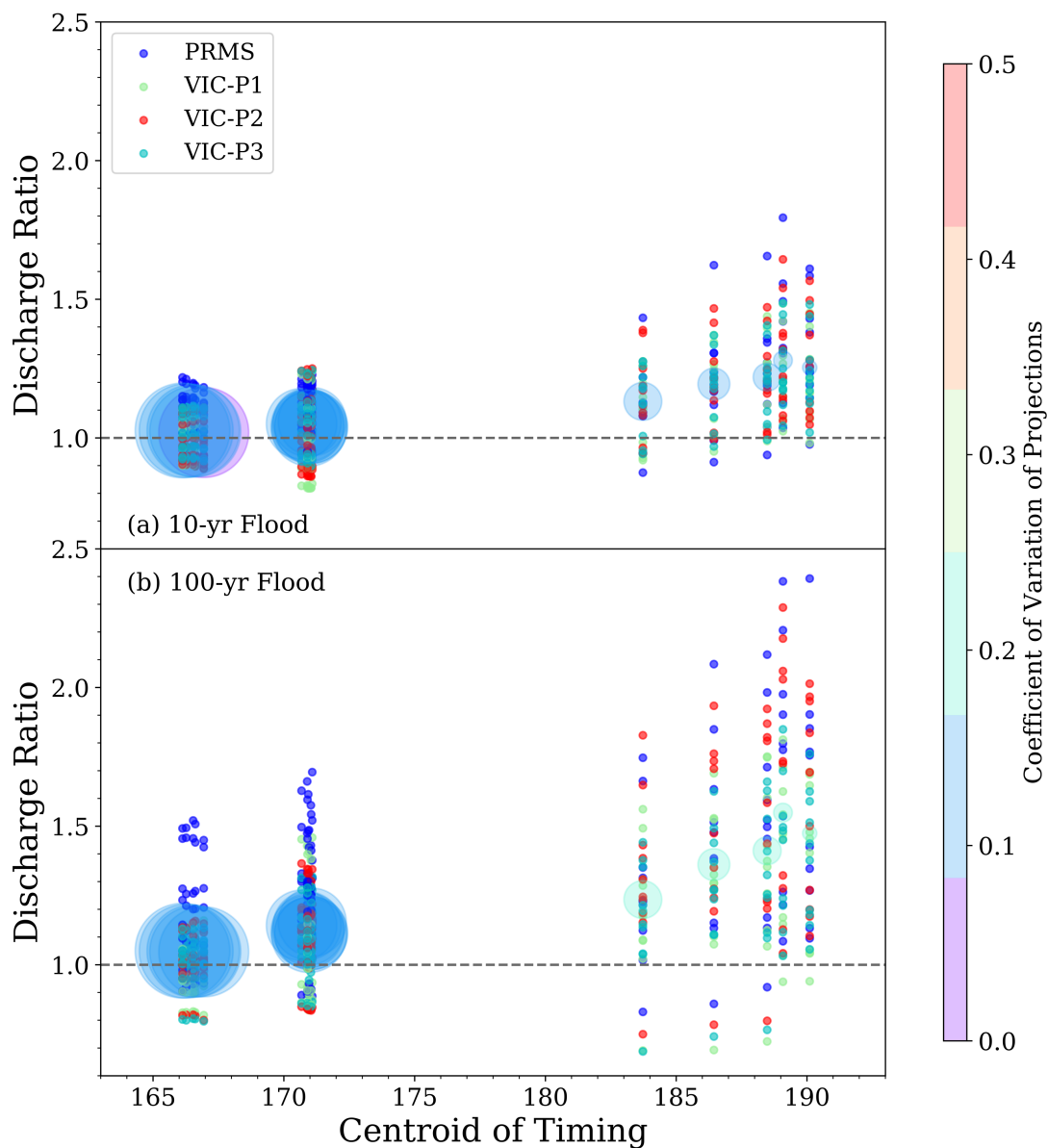
474

475

476 **Figure 3.** Discharge ratios (future:past) versus centroid of timing (day on which 50% of water-year flow has  
477 passed, an indicator of snow dominance) for all 396 locations and four return periods. For each location, the  
478 average of 40 ensemble member ratios calculated from GEV distribution fitting from 50-year windows for the  
479 future (2050-2099) and past (1950-1999) time periods is shown. Points are sized by average daily streamflow and  
480 colored by the coefficient of variation of the 40 ratios.

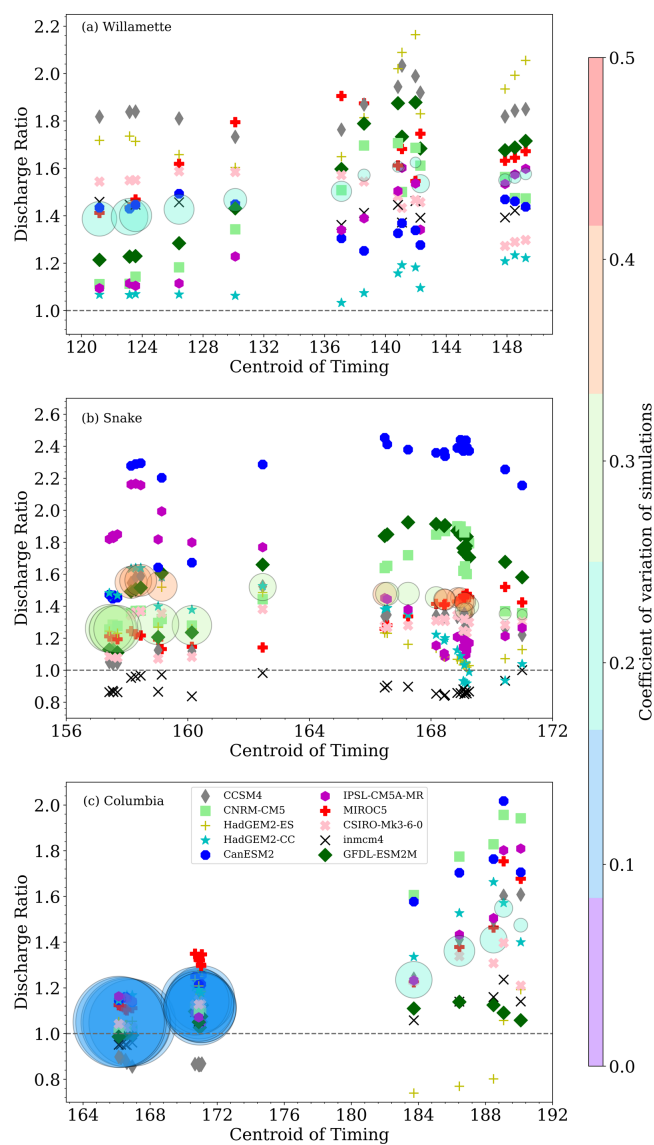


481  
 482 **Figure 4.** As in Figure 3 but only for points on the indicated rivers. Dashed lines indicate tributaries: 9-12 are on  
 483 the Middle Fork Willamette, 15-17 on the McKenzie; tributaries of the Snake are the Grand Ronde (14),  
 484 Clearwater (17) and Salmon (24). In the lower panel, the Grand Ronde and Salmon are clearly distinguished by a  
 485 black circle around their perimeter. Table 1 translates the codes in the legend into named locations and shows the  
 486 numerical values represented in the figure. As is evident from both snow-dominance and size, locations are  
 487 ordered downstream to upstream from left to right for each river.

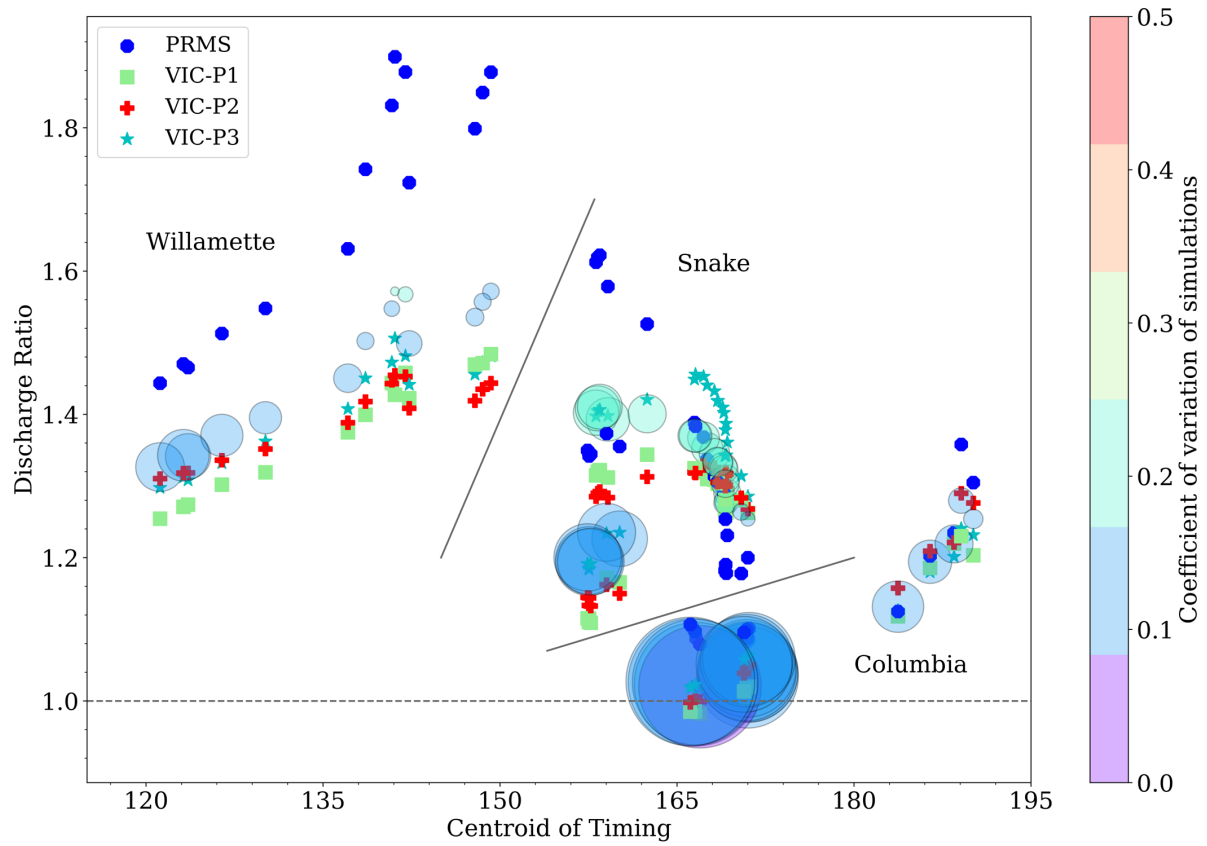


488

489 **Figure 5.** Averaged (large circles) and individual ensemble member (small colored circles) discharge ratios for  
490 simulated streamflow locations along the mainstem Columbia River for the 10-year (top) and 100-year (bottom)  
491 return periods. As shown in the legend, the color of the dots distinguishes results by hydrologic model setup.



492 **Figure 6.** Average ratios of all 40 ensemble members (large circles) and the average of 4 hydrologic model  
493 results for each GCM (symbols), shown for simulated streamflow locations along the Willamette (top), Snake  
494 (middle), and the mainstem Columbia (bottom) for 100-year return periods. GCMs are ordered in the legend  
495 by their ranking in Rupp et al. (2017), representing their ability to simulate Northwest climate.

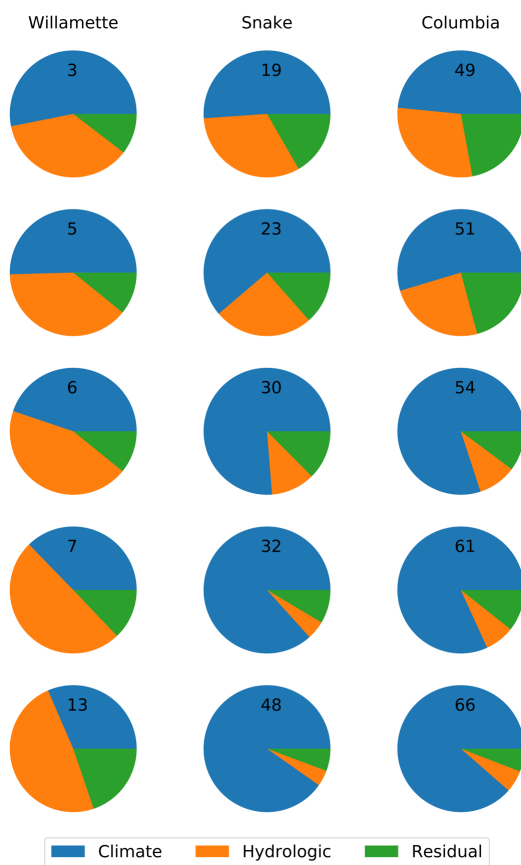


496

497

498 **Figure 7:** as in Figure 6 but averaged by hydrologic model, for 10-year return period, and combined into one  
499 panel.





500 **Figure 8.** ANOVA results for select locations on the indicated rivers, for climate and hydrologic factors (and the  
501 residual). Charts are numbered to correspond with their location in Figure 4, with the most-downstream location  
502 at the top.



503

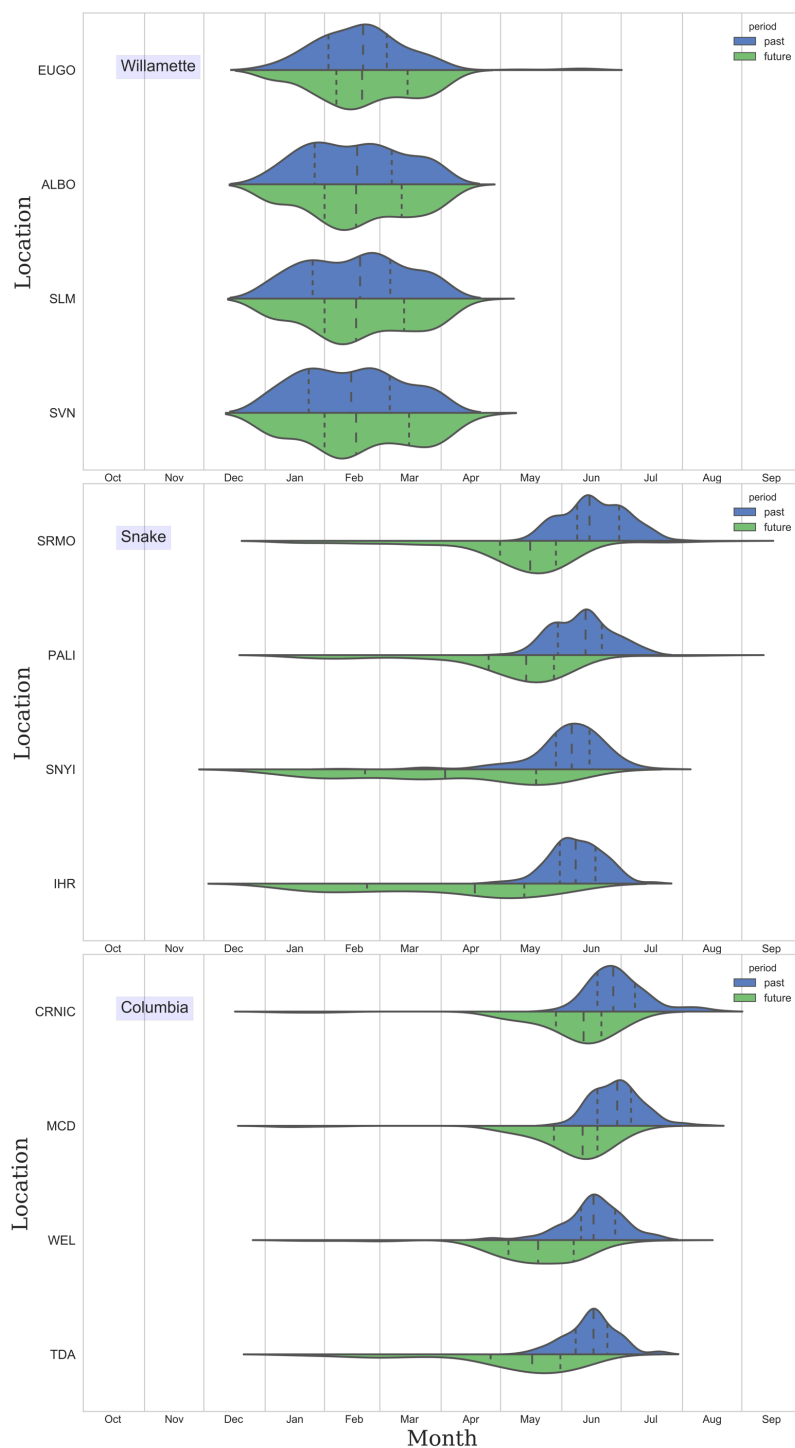


**Figure 9.** Statistical representations of the variation through the water year of the timing of flood events. For each of the 40 simulations, the dates of the 5 highest flows in the 50-year past (blue) and future (green) windows are tallied, and the resulting distributions smoothed. Long dashed lines indicate median date, short dashed lines the lowest and highest quartiles.



504

505 **Table 1 Information about locations featured in this paper - location, river, and discharge ratios**

River	UW Key	Description	10-year flood discharge ratios				100-year flood discharge ratios			
			Avg.	Coeff. of Var.	Min	Max	Avg.	Coeff. of Var.	Min	Max
Chehalis	CHEGR	Chehalis R nr Grand Mount	1.21	0.09	1.0 <sub>3</sub>	1.42	1.34	0.18	0.87	2.07
Chehalis	CHE	Chehalis R at Porter	1.21	0.08	1.0 <sub>3</sub>	1.40	1.31	0.16	0.91	1.89
Willamette	SVN	T.W. Sullivan	1.33	0.09	1.0 <sub>7</sub>	1.64	1.39	0.22	0.87	2.39
Willamette	WILPO	Portland	1.34	0.09	1.0 <sub>8</sub>	1.69	1.40	0.23	0.86	2.47
Willamette	WILLA	Newberg	1.34	0.09	1.0 <sub>9</sub>	1.66	1.40	0.22	0.88	2.44
Willamette	SLM	Salem	1.37	0.09	1.1 <sub>0</sub>	1.70	1.43	0.22	0.84	2.52
Willamette	ALBO	Albany	1.40	0.09	1.1 <sub>1</sub>	1.73	1.47	0.20	0.89	2.40
Willamette	HARO	Harrisburg	1.45	0.10	1.1 <sub>8</sub>	1.86	1.50	0.22	0.88	2.37
Willamette	JASO	Middle fork @ Jasper	1.50	0.14	1.2 <sub>0</sub>	2.13	1.57	0.23	0.93	2.68
Willamette	DEX	Dexter	1.55	0.16	1.1 <sub>7</sub>	2.33	1.61	0.22	1.05	2.67
Willamette	HCR	Hills Creek	1.57	0.18	1.1 <sub>5</sub>	2.46	1.60	0.25	1.10	3.18
Willamette	WILNF	Oakridge	1.57	0.18	1.1 <sub>6</sub>	2.45	1.63	0.24	1.09	2.88
Willamette	EUGO	WR at Eugene (NWP)	1.50	0.12	1.2 <sub>6</sub>	2.04	1.54	0.22	0.88	2.57
Willamette	WAV	Walterville	1.54	0.13	1.2 <sub>9</sub>	2.13	1.55	0.18	1.04	2.23
Willamette	LEA	Leaburg	1.56	0.14	1.2 <sub>8</sub>	2.23	1.56	0.18	1.05	2.34
Willamette	VIDO	McKenzie nr Vida	1.57	0.15	1.2 <sub>8</sub>	2.32	1.58	0.19	1.02	2.41
Willamette	COT	Cottage Grove	1.25	0.11	0.9 <sub>7</sub>	1.69	1.39	0.29	0.78	2.38



River	UW Key	Description	10-year flood discharge ratios				100-year flood discharge ratios			
			Avg.	Coeff. of Var.	Min	Max	Avg.	Coeff. of Var.	Min	Max
Snake	IHR	Ice Harbor	1.20	0.13	0.9 2	1.75	1.26	0.28	0.79	2.84
Snake	LMN	Lower Monumental	1.20	0.13	0.9 2	1.76	1.26	0.28	0.78	2.77
Snake	LGS	Little Goose	1.19	0.13	0.9 2	1.77	1.26	0.28	0.78	2.83
Snake	LWG	Lower Granite	1.19	0.13	0.9 2	1.77	1.25	0.29	0.78	2.89
Snake	ANA	Anatone	1.24	0.14	0.9 5	1.74	1.29	0.29	0.78	2.84
Snake	LIM	Lime Point	1.23	0.14	0.9 4	1.73	1.28	0.30	0.76	2.81
Snake	HCD	Hells Canyon	1.40	0.18	1.0 1	2.11	1.55	0.38	0.87	3.62
Snake	OXB	Oxbow	1.41	0.18	1.0 1	2.11	1.56	0.38	0.86	3.65
Snake	BRN	Brownlee Dam	1.41	0.18	1.0 1	2.12	1.56	0.37	0.86	3.63
Snake	WEII	Weiser, ID	1.39	0.18	1.0 2	2.09	1.53	0.35	0.86	3.28
Snake	SNYI	Nyssa, OR	1.40	0.18	1.0 4	2.16	1.52	0.33	0.89	3.21
Snake	SWAI	Murphy, ID	1.37	0.19	0.9 8	2.09	1.48	0.33	0.84	3.24
Snake	CJSTR	CJ Strike Dam	1.37	0.19	0.9 7	2.08	1.48	0.32	0.86	3.08
Snake	SKHI	King Hill, ID	1.37	0.19	0.9 6	2.08	1.48	0.32	0.85	2.84
Snake	SNKBL WLSAL MON	Hagerman, ID	1.35	0.18	0.9 3	2.05	1.46	0.31	0.83	2.66
Snake	BUHL	Buhl, ID	1.35	0.19	0.9 1	2.05	1.46	0.32	0.73	2.54
Snake	KIMI	Kimberly, ID	1.33	0.19	0.8 9	2.03	1.44	0.33	0.74	2.47
Snake	MILI	Milner, ID	1.33	0.19	0.8 8	2.04	1.44	0.34	0.73	2.52



River	UW Key	Description	10-year flood discharge ratios				100-year flood discharge ratios			
			Avg.	Coeff. of Var.	Min	Max	Avg.	Coeff. of Var.	Min	Max
Snake	MINI	Minidoka, ID	1.33	0.19	0.86	2.02	1.45	0.33	0.70	2.53
Snake	AMFI	Neeley American Falls	1.32	0.19	0.85	1.99	1.45	0.34	0.67	2.69
Snake	BFTI	nr Blackfoot, ID	1.31	0.19	0.84	1.96	1.43	0.34	0.67	2.72
Snake	SNAI	nr Blackfoot, ID	1.30	0.19	0.84	1.95	1.43	0.34	0.67	2.69
Snake	SHYI	Shelley, ID	1.29	0.18	0.84	1.92	1.40	0.33	0.69	2.62
Snake	LORI	Lorenzo, ID	1.28	0.19	0.86	1.91	1.38	0.34	0.69	2.52
Snake	HEII	Heise, ID	1.28	0.18	0.86	1.91	1.37	0.33	0.70	2.53
Snake	PALI	Irwin Palisades	1.28	0.19	0.87	1.95	1.37	0.34	0.71	2.60
Snake	JKSY	Jackson, WY	1.26	0.15	0.89	1.73	1.35	0.30	0.80	2.46
Snake	SRMO	Moose, WY	1.25	0.13	0.91	1.59	1.35	0.25	0.83	2.34
Grand Ronde	TRY	Troy	1.48	0.19	1.09	2.55	1.68	0.34	1.01	4.38
Salmon	WHB	White Bird	1.07	0.13	0.83	1.57	1.09	0.33	0.72	2.81
Columbia	CRVAN	Vancouver	1.03	0.09	0.90	1.22	1.05	0.13	0.80	1.49
Columbia	BON	Bonneville	1.03	0.09	0.90	1.21	1.05	0.13	0.80	1.49
Columbia	TDA	The Dalles	1.03	0.08	0.90	1.20	1.05	0.13	0.81	1.52
Columbia	JDA	John Day	1.02	0.08	0.90	1.19	1.05	0.13	0.80	1.51
Columbia	MCN	McNary Dam	1.02	0.08	0.89	1.18	1.05	0.13	0.80	1.45
Columbia	CLKEN	Clover Island @ Kennewick	1.03	0.10	0.82	1.22	1.11	0.14	0.84	1.49



River	UW Key	Description	10-year flood discharge ratios				100-year flood discharge ratios			
			Avg.	Coeff. of Var.	Min	Max	Avg.	Coeff. of Var.	Min	Max
Columbia	CHJ	Chief Joseph	1.06	0.11	0.8 <sub>3</sub>	1.25	1.15	0.15	0.85	1.70
Columbia	GCL	Grand Coulee	1.06	0.11	0.8 <sub>3</sub>	1.25	1.14	0.14	0.84	1.66
Columbia	PRD	Priest Rapids	1.04	0.10	0.8 <sub>2</sub>	1.22	1.11	0.13	0.84	1.54
Columbia	WAN	Wanapum	1.04	0.10	0.8 <sub>2</sub>	1.22	1.11	0.14	0.84	1.58
Columbia	RIS	Rock Island	1.04	0.10	0.8 <sub>2</sub>	1.23	1.12	0.14	0.84	1.60
Columbia	RRH	Rocky Reach	1.05	0.10	0.8 <sub>3</sub>	1.23	1.13	0.14	0.84	1.61
Columbia	WEL	Wells Dam	1.05	0.10	0.8 <sub>3</sub>	1.24	1.14	0.14	0.85	1.63
Columbia	ARD	Hugh Keenleyside (Arrow)	1.13	0.12	0.8 <sub>7</sub>	1.43	1.24	0.21	0.69	1.83
Columbia	RVC	Revelstoke	1.19	0.12	0.9 <sub>1</sub>	1.62	1.36	0.23	0.69	2.08
Columbia	MCD	Mica Dam	1.22	0.12	0.9 <sub>4</sub>	1.66	1.41	0.24	0.72	2.12
Columbia	DONAL	Donald	1.28	0.14	1.0 <sub>2</sub>	1.79	1.55	0.25	0.94	2.38
Columbia	CRNIC	Nicholson	1.25	0.13	0.9 <sub>8</sub>	1.61	1.47	0.23	0.94	2.39
Clearwater	SPD	Spalding, ID	1.15	0.15	0.8 <sub>5</sub>	1.78	1.32	0.30	0.80	2.63
Clearwater	DWR	Dworshak Dam, ID	1.14	0.12	0.8 <sub>6</sub>	1.55	1.30	0.24	0.89	2.22
Santiam	JFFO	Santiam R nr Jefferson	1.40	0.10	1.1 <sub>4</sub>	1.81	1.41	0.25	0.81	2.27
Kootenay	COR	Corra Linn Dam, BC	1.08	0.12	0.8 <sub>5</sub>	1.31	1.15	0.16	0.79	1.67
Kootenai	LIB	Libby Dam, MT	1.17	0.14	0.9 <sub>2</sub>	1.52	1.32	0.22	0.85	2.01
Kootenay	BFE	Bonner's Ferry, ID	1.13	0.13	0.8 <sub>9</sub>	1.45	1.26	0.20	0.83	2.02



River	UW Key	Description	10-year flood discharge ratios				100-year flood discharge ratios			
			Avg.	Coeff. of Var.	Min	Max	Avg.	Coeff. of Var.	Min	Max
Pend Oreille	ALF	Albeni Falls, ID	1.26	0.14	0.96	1.68	1.65	0.30	1.02	2.97
Flathead	CFM	Columbia Falls, MT	1.24	0.13	0.94	1.63	1.65	0.26	1.01	3.19
Flathead	HGH	Hungry Horse Dam, MT	1.30	0.13	1.04	1.70	1.78	0.29	1.16	3.56
Yakima	KIOW	Yakima, WA	1.82	0.21	1.35	3.11	2.28	0.30	1.57	4.39

506